Montes Taurus J. Pure Appl. Math. 6 (3), 558–578, 2024

Montes Taurus Journal of Pure and Applied Mathematics

https://www.mtjpamjournal.com

MTJPAM
ISSN: 2687-4814

Stability analysis of SIRI epidemic model with reintroduced susceptibles under incorporated time delay on susceptible individuals

Kanaka Maha Lakshmi Emandi [a], Kalesha Vali Shaik [b], Appa Rao Dokala [c], Salma Umme [d]

[a] *Department of Engineering Mathematics, Andhra University, 530003 Visakhapatnam, India*
[b] *Department of Engineering Mathematics, Andhra University, 530003 Visakhapatnam, India*
[c] *Department of Mathematics, Indian Institutes of Information Technology (IIIT), Rajiv Gandhi University of Knowledge Technologies (RGUKT), 532402 Srikakulam, India*
[d] *Department of Electrical Electronics and Communication Engineering (EECE), Gandhi Institute of Technology and Management (GITAM) University, 530045 Visakhapatnam, India*

Abstract

In this paper, a three-compartment SIRI epidemic model with reintroduced susceptibles under incorporated time delay on susceptible individuals is considered. Determined disease free, endemic equilibrium points and discussed local stability at endemic equilibrium point. Identified the point where the system stabilizes by means of Hopf bifurcation. Ascertained the results by numerical simulation using MATLAB. Observed that the system becomes unstable in both the cases of increase in the transmission rate and additional transaction rate respectively at a fixed critical time delay parameter using numerical examples.

Keywords: Re-infection rate, additional transaction rate, disease free equilibrium point, endemic equilibrium point, time delay, critical time delay parameter, Hopf-bifurcation

2020 MSC: 92D25, 92D30, 93Dxx, 93D05

1. Introduction

An epidemic is the fast change of location of a disease that affects a large percentage of the population in a certain area. Epidemiology is the study of epidemics. A mathematical model is a creation of a real-world system or process through mathematical ideas and principles such as variables, equations, and functions to describe and analyze its behavior. These models aim to simplify complex systems by capturing essential relationships and dynamics in a mathematical form. The key components of a mathematical model include variables (which represent changing quantities), parameters (which are fixed values), and equations that describe the interactions between variables. Mathematical models are widely used in various fields such as physics, engineering, economics, biology, and social sciences. In

†*Article ID:* MTJPAM-D-24-00155

Email addresses: kanakamahalakshmmi.rs@andhrauniversity.edu.in (Kanaka Maha Lakshmi Emandi), prof.skvali@andhrauniversity.edu.in (Kalesha Vali Shaik), appuhcu.2007@gmail.com (Appa Rao Dokala), usalma123@gmail.com (Salma Umme)

Received:25 September 2024, Accepted:14 February 2025, Published:12 August 2025

⋆*Corresponding Author:* Kanaka Maha Lakshmi Emandi

This work is licensed under a Creative Commons Attribution 4.0 International License.

physics, they are used to describe forces and motion (e.g., Newton's laws), while in economics, they help analyze market behaviors or optimize resource allocation. In biology, mathematical models explain population dynamics or the spread of diseases through epidemiological models like SIR. Environmental science uses models to predict climate change and pollution spread, while operations research applies mathematical models to optimize logistics and production processes. Furthermore, machine learning models, which are based on mathematical algorithms, are used in artificial intelligence for tasks such as classification, prediction, and decision-making. Ultimately, mathematical models are essential tools for understanding, predicting, and controlling real-world systems and phenomena.

Among the various epidemiological models, the SIS and SIR models are considered the most effective and extensively studied. Dokala et al. [2]-[7] have conducted in-depth analyses on the stability of these SIR models. Subsequently, Gummala et al. [10], explored the stability of the SIR epidemic model, particularly under vaccination coverage for newborns. They also examined the dynamics of delays by incorporating time delays in the interactions between susceptible and infected individuals (*cf.* [11]). The SIR model can be made more complex by incorporating several infection stages, age structure, and spatial variability, among other things. The SIRI model is one such extension. The book "Population Biology and Criticality" covers partial immunity models, also known as Susceptible-Infected-Recovered-Infected (SIRI) models (*cf.* [13]). David [1] created an epidemiological model for a community using SIRI. The three compartments in this paradigm are identified by the letters S, I, and R: susceptible, infectious, and removed people. This theory states that removable persons have three phases in their life cycle: infectious, immune-mediated, and infectious again. The SIRI paradigm is applicable to certain disorders, including as herpes and tuberculosis in humans and animals (*cf.* [12, 14, 15]), where recovered individuals may relapse into the infectious class due to inadequate treatment or the reactivation of a latent infection. This type of SIRI pandemic model has been studied by certain authors in order to comprehend the theory behind illness spread. As a result, a large number of mathematicians and scientists started focusing on SIRI epidemic models to better understand disease transmission. Time delays were introduced to account for various factors influencing how the disease spreads within the population. Emandi et al. [8] explored the stability of the SIRI epidemic model with the reintroduction of susceptibles, assuming a constant population, and applied analytical methods. They also examined the delay dynamics of the same model, incorporating time delays in the interactions between susceptible and infected individuals, and found that an increase in the transmission rate leads to system instability (*cf.* [9]). The term "time delay" in epidemic models describes the incorporation of lags or delays in the transitions between the model's various compartments. Individuals are sometimes classified into several categories or compartments in compartmental epidemic models according to their disease status, such as susceptible (S), infected (I), and recovered (R). Time delays in the susceptible population are included in mathematical models of infectious illness dissemination to better represent the dynamics of disease transmission. The concept of time delay in the susceptible population refers to the time it takes for susceptible individuals to transition into the infectious compartment after exposure to the infectious agent. This enables the model to account for the lag between exposure and infectiousness, which can have implications for predicting the course of an epidemic, estimating the effectiveness of control measures, and understanding the impact of interventions such as vaccination or quarantine. Reducing the initial spread of the disease by introducing a temporal delay for the susceptible population. This is due to the fact that people exposed to the disease do not spread the infection right away, which lowers the rate of transmission.

In the second section, governing equations are formed by incorporating time delay in the susceptible individuals and by choosing suitable parameters and variables. In the third section, derived the steady state points from governing equations. In the fourth section, discussed the local stability at endemic equilibrium point and identified the conditions at which the system becomes stable. In the fifth section, identified the critical point where the stability of the system switches by using Hopf bifurcation. In the sixth section, an attempt is made to ascertained the results by numerical simulation using MATLAB. Also to observe the stability of the system with respective to transmission and additional transaction rates numerical examples are considered and it is observed that the system becomes unstable in both the cases of increase in the transmission rate and additional transaction rate at a fixed critical time delay parameter.

2. Basic equations of the model

Stollenwerk and Jansen [13] discussed the partial immunity models, in specific discussed (Susceptible - infected - recovered - infected) SIRI models (*cf.* [13]). The SIRI epidemic model is essential for understanding how diseases spread within populations. By categorizing individuals into susceptible, infected, recovered, and isolated groups, it

helps predict transmission dynamics. Writing the basic equations of this model aids in analyzing disease progression, guiding public health decisions, and optimizing control strategies for outbreaks. We considered one of such models in which a three-compartment SIRI model with reintroduced susceptibles i.e., SIR$^{\nearrow \mathrm{I}}_{\searrow \mathrm{S}}$ model in one of our paper (*cf.* [9]) and discussed in detail by incorporating delay in the interaction of susceptible and infected individuals. In this paper, the same model with time delay incorporated in susceptible individuals is considered. The flowchart of the model is presented in Figure 1 based on the model's assumptions. The transit of people between the model compartments can be seen in this flow chart. The description of variables and parameters that are considered in [9] are presented for ready reference Tables 1 and 2.

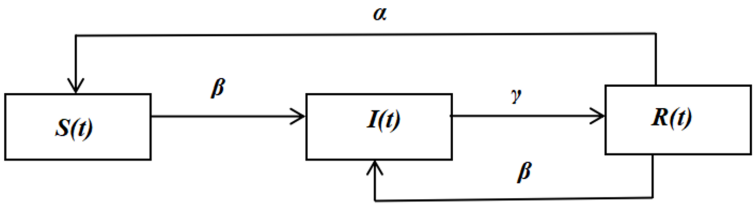

Figure 1. Flowchart demonstrating how people travel across the model compartments

Variable	Description
$S(t)$	Susceptible individuals with respective to time t
$I(t)$	Infected individuals with respective to time t
$R(t)$	Recovered individuals with respective to time t

Table 1. Variables and its description

Parameter	Description
β	Rate of infection or Reinfection rate
γ	Recovery rate of infected individual
α	The additional rate at which recovered individuals (R) return to the susceptible (S) class
τ	Parameter for time delay
τ_0	Critical time delay parameter or Bifurcation point

Table 2. Parameters and its description

Using the model assumptions, we formulated the governing equations of the model are

$$\begin{aligned} \frac{dS}{dt} &= \alpha R - \beta S(t-\tau)I, \\ \frac{dI}{dt} &= \beta S(t-\tau)I - \gamma I + \beta RI, \\ \frac{dR}{dt} &= \gamma I - \alpha R - \beta RI. \end{aligned} \tag{2.1}$$

3. Steady-state points

In understanding the disease dynamics, equilibrium points play a vital role. Hence, an attempt is made to identify disease-free and endemic equilibrium points using the governing equations in (2.1). The disease-free equilibrium

represents when no infection exists, while the endemic equilibrium shows long-term disease persistence. Analyzing both helps guide intervention strategies and predict future outbreak trends. In this section, the equilibrium points, namely a disease-free equilibrium point, and endemic equilibrium point are determined by solving the equations in (2.1) after equating them individually to zero. i.e.,

$$\frac{dS}{dt} = 0, \frac{dI}{dt} = 0, \frac{dR}{dt} = 0.$$

The equilibrium points are as follows:

E_1 : Disease free equilibrium point is

$$E_1(S^*, I^*, R^*) = (N, 0, 0). \tag{3.1}$$

E_2 : Endemic equilibrium point is

$$E_2(S^*, I^*, R^*) = \left(\frac{\alpha(\beta\gamma N - \gamma^2)}{\beta(\alpha + \beta N - \gamma)(\beta N - \gamma)}, \frac{\beta N - \gamma}{\beta}, \frac{\beta\gamma N - \gamma^2}{\beta(\alpha + \beta N - \gamma)}\right). \tag{3.2}$$

Here, the basic reproduction rate of the system (2.1) is identified as $R_0 = \frac{\beta N}{\gamma}$. Also it is observed that if $R_0 > 1$, the endemic equilibrium point exist and if $R_0 < 1$ the system has no feasible solution.

4. Stability at equilibrium points

To predict long term disease behavior in epidemic models, the stability at endemic equilibrium point is essential. Stability analysis helps to determine whether the disease will persist or decline. The analysis guides effective public health interventions and strategies to control and manage ongoing disease spread in populations. In this section, we prove that the system is asymptotically stable at the endemic equilibrium point E_2 subject to the condition stated in the following theorem. Stability is studied even when time delay is introduced in the susceptible individuals and identified the point at which the system becomes unstable to stable using Hopf bifurcation.

Theorem 4.1. *The system* (2.1) *is locally asymptotically stable at endemic equilibrium point* $E_2(S^*, I^*, R^*)$.

Proof. Let us represents the equations in (2.1) individually as $g_1,\ g_2,\ g_3$. That is

$$\begin{aligned} g_1 &= \alpha R - \beta S(t-\tau)I, \\ g_2 &= \beta S(t-\tau)I - \gamma I + \beta RI, \\ g_3 &= \gamma I - \alpha R - \beta RI. \end{aligned} \tag{4.1}$$

The Jocobian matrix for the above system (4.1) is

$$J = \begin{bmatrix} \frac{\partial g_1}{\partial S} & \frac{\partial g_1}{\partial I} & \frac{\partial g_1}{\partial R} \\ \frac{\partial g_2}{\partial S} & \frac{\partial g_2}{\partial I} & \frac{\partial g_2}{\partial R} \\ \frac{\partial g_3}{\partial S} & \frac{\partial g_3}{\partial I} & \frac{\partial g_3}{\partial R} \end{bmatrix}.$$

Hence,

$$J = \begin{bmatrix} -\beta e^{-\lambda\tau} I & -\beta S & \alpha \\ \beta e^{-\lambda\tau} I & \beta S - \gamma + \beta R & \beta I \\ 0 & \gamma - \beta R & -\alpha - \beta I \end{bmatrix}.$$

The Jacobean matrix for the system (4.1) at endemic equilibrium point $E_2(S^*, I^*, R^*)$ is

$$J = \begin{bmatrix} -\beta e^{-\lambda\tau} I^* & -\beta S^* & \alpha \\ \beta e^{-\lambda\tau} I^* & \beta S^* - \gamma + \beta R^* & \beta I^* \\ 0 & \gamma - \beta R^* & -\alpha - \beta I^* \end{bmatrix}. \tag{4.2}$$

The characteristic equation of (4.2) with λ as a parameter is given by

$$|J - \lambda I| = 0$$

$$\lambda^3 + \lambda^2(\gamma + \alpha + \beta(I^* - (S^* + R^*))) + \lambda(\alpha\gamma - \beta\alpha(S^* + R^*) - \beta^2 S^* I^*)$$
$$+e^{-\lambda\tau}[\lambda^2(\beta I^*) + \lambda(\beta\gamma I^* + \alpha\beta I^* + \beta^2 I^*(I^* - (S^* + R^*)) + \beta^2 S^* I^*)] = 0$$

i.e.,

$$\varphi(\lambda, \tau) = \lambda^3 + u_1\lambda^2 + u_2\lambda + e^{-\lambda\tau}(v_1\lambda^2 + v_2\lambda) = 0, \tag{4.3}$$

where

$$u_1 = \gamma + \alpha + \beta(I^* - (S^* + R^*)),$$
$$u_2 = \alpha\gamma - \beta\alpha(S^* + R^*) - \beta^2 S^* I^*,$$
$$v_1 = \beta I^*,$$
$$v_2 = \beta\gamma I^* + \alpha\beta I^* + \beta^2 I^*(I^* - (S^* + R^*)) + \beta^2 S^* I^*.$$

To find the condition for existence of negative real roots of (4.3),

Case (i): For $\tau = 0$, the equation (4.3) becomes

$$\begin{aligned} \varphi(\lambda, 0) &= \lambda[\lambda^2 + \lambda(\gamma + \alpha + \beta I^* + \beta(I^* - (S^* + R^*))) + (\alpha\gamma + \beta\gamma I^* + \alpha\beta(I^* - (S^* + R^*)) \\ &\quad +\beta^2 I^*(I^* - (S^* + R^*)))] \\ &= 0 \end{aligned} \tag{4.4}$$

which gives that

$$\lambda = 0$$

or

$$\lambda^2 + \lambda(\gamma + \alpha + \beta I^* + \beta(I^* - (S^* + R^*))) + (\alpha\gamma + \beta\gamma I^* + \alpha\beta(I^* - (S^* + R^*)) + \beta^2 I^*(I^* - (S^* + R^*))) = 0. \tag{4.5}$$

Thus, one of the roots of (4.4) is zero and the system is stable if equation (4.5) possesses negative real roots. Here

$$\frac{-(\gamma + \alpha + \beta I^* + \beta(I^* - (S^* + R^*)))}{1} < 0 \text{ if } 2I^* > N \text{ and}$$

$$\frac{\alpha\gamma + \beta\gamma I^* + \alpha\beta(I^* - (S^* + R^*)) + \beta^2 I^*(I^* - (S^* + R^*))}{1} > 0 \text{ if } 2I^* > N.$$

Therefore, the system (2.1) is locally asymptotically stable at endemic equilibrium point $E_2(S^*, I^*, R^*)$, if $2I^* > N$.

Case (ii): For $\tau > 0$, there exists a positive τ_0 such that the equation (4.3) has pair of purely imaginary roots, and can be taken as $\pm i\omega$, $\omega > 0$.

Since equation (4.3) is a transcendental equation, Routh-Hurwitz criterion cannot be applied to find the roots of the equation. So, by Rouche's theorem, the transcendental equation shall have positive real part only, when the equation has purely imaginary roots.

Let $\lambda = \pm i\omega$ be a purely imaginary roots of the equation (4.3). Then (4.3) becomes

$$(i\omega)^3 + u_1(i\omega)^2 + u_2(i\omega) + e^{-i\omega\tau}(v_1(i\omega)^2 + v_2(i\omega)) = 0,$$

$$(-\omega^2 u_1 - v_1\omega^2\cos(\omega\tau) + v_2\omega\sin(\omega\tau)) + i(-\omega^3 + \omega u_2 + v_2\omega\cos(\omega\tau) + v_1\omega^2\sin(\omega\tau)) = 0.$$

Separating real and imaginary parts we get the following two equations

$$v_2\omega\sin(\omega\tau) - v_1\omega^2\cos(\omega\tau) = \omega^2 u_1, \tag{4.6}$$

$$v_2\omega\cos(\omega\tau) + v_1\omega^2\sin(\omega\tau) = \omega^3 - \omega u_2. \tag{4.7}$$

On adding, the equations (4.6) and (4.7) after squaring, we get

$$(v_1\omega^2)^2 + (v_2\omega)^2 = (\omega^2 u_1)^2 + (\omega^3 - \omega u_2)^2 \tag{4.8}$$

i.e.,

$$\omega^6 + \omega^4(u_1^2 - 2u_2 - v_1^2) + \omega^2(u_2^2 - v_2^2) = 0.$$

Let

$$\psi(t) = t^3 + t^2 M_1 + tM_2 = 0,$$

where

$$M_1 = u_1^2 - 2u_2 - v_1^2, M_2 = u_2^2 - v_2^2, t = \omega^2. \tag{4.9}$$

Therefore $\psi(t) = 0$.

If we assume that $M_1 > 0, M_2 > 0$ then equation (4.9) have no positive real roots.

Therefore the equation (4.9) admits negative real roots. Hence, we can derive the conditions for existences of stability at endemic equilibrium point. □

Theorem 4.2. *The system is locally asymptotically stable for all τ, at endemic equilibrium E_2 if following conditions hold:*

$$\textbf{(i)}\quad R_0 > 1, \qquad \textbf{(ii)}\ (u_1 + v_1) > 0, (u_2 + v_2) > 0, \qquad \textbf{(iii)}\ M_1 > 0, M_2 > 0.$$

Proof. Let any one of M_1, M_2 is negative then equation (4.9) has a positive root ω_0. From the equation (4.6) and (4.7) and by Cramer's rule, we have

$$\cos(\omega\tau) = \frac{\begin{vmatrix} \omega^2 u_1 & v_2\omega \\ \omega^3 - \omega u_2 & v_1\omega^2 \end{vmatrix}}{\begin{vmatrix} -v_1\omega^2 & v_2\omega \\ v_2\omega & v_1\omega^2 \end{vmatrix}},$$

i.e.,

$$\cos(\omega\tau) = \frac{\omega^4(v_2 - u_1v_1) - \omega^2 u_2 v_2}{v_1^2\omega^4 + v_2^2\omega^2}$$

or

$$\tau_k = \frac{1}{\omega_0}\cos^{-1}\left(\frac{\omega_0^2(v_2 - u_1v_1) - u_2v_2}{v_1^2\omega_0^2 + v_2^2}\right) + \frac{2k\pi}{\omega_0},$$

where $k = 0, 1, 2, 3, \ldots$. □

5. Hopf-bifurcation

A critical point where the system stability switches, and periodic solution arise is called Hopf-bifurcation. Bifurcation analysis helps identifing critical thresholds where disease dynamics change drastically. The Hopf-bifurcation method allows us to figure out when the disease shifts from persistence to eradication, guiding the development of effective control strategies and interventions. Generally, the system losses its stability i.e., the system becomes unstable due to unbounded periodic oscillations arise at this critical point. Hopf-bifurcation takes place when a pair of complex conjugate eigen values cross the imaginary axis around the equilibrium points. Hopf-bifurcation exists for the system when it is characterized by the system of ordinary differential equations. The following theorem establishes the existence of Hopf-bifurcation for the three-dimensional system with time delay.

Theorem 5.1. *If $R_0 > 1$ there exist a positive τ_0 such that the following results hold*

(i) *If $0 < \tau < \tau_0$, the system of equations* (2.1) *is locally asymptotically stable at endemic equilibrium point E_2.*

(ii) *The system* (2.1) *exhibits a Hopf-bifurcation if $\tau > \tau_0$.*

Proof. To obtain Hopf-bifurcation, we need to check the transversal condition for the existence of complex eigen value at $\tau = \tau_0$. i.e., the real part of $\lambda(\tau)$ become positive when $\tau > \tau_0$. At this stage, the stable state become unstable. That is the system exhibits Hopf-bifurcation when τ crosses the critical value τ_0.

Differentiating (4.3) with respect to τ, we get

$$3\lambda^2\frac{d\lambda}{d\tau} + 2u_1\lambda\frac{d\lambda}{d\tau} + u_2\frac{d\lambda}{d\tau} + e^{-\lambda\tau}(2v_1\lambda\frac{d\lambda}{d\tau} + v_2\frac{d\lambda}{d\tau}) + (v_1\lambda^2 + v_2\lambda)(-\lambda - \tau\frac{d\lambda}{d\tau})e^{-\lambda\tau} = 0,$$

i.e.,

$$\frac{d\lambda}{d\tau}[3\lambda^2 + 2u_1\lambda + u_2 + e^{-\lambda\tau}(2v_1\lambda + v_2) - (v_1\lambda^2 + v_2\lambda)\tau e^{-\lambda\tau}] = (v_1\lambda^2 + v_2\lambda)\lambda e^{-\lambda\tau}$$

or

$$\left(\frac{d\lambda}{d\tau}\right)^{-1} = \frac{[3\lambda^2 + 2u_1\lambda + u_2 + e^{-\lambda\tau}(2v_1\lambda + v_2) - (v_1\lambda^2 + v_2\lambda)\tau e^{-\lambda\tau}]}{(v_1\lambda^2 + v_2\lambda)\lambda e^{-\lambda\tau}},$$

$$\left(\frac{d\lambda}{d\tau}\right)^{-1} = \frac{[3\lambda^2 + 2u_1\lambda + u_2]}{(v_1\lambda^2 + v_2\lambda)\lambda e^{-\lambda\tau}} + \frac{(2v_1\lambda + v_2)}{(v_1\lambda^2 + v_2\lambda)\lambda} - \frac{\tau}{\lambda},$$

$$\left(\frac{d\lambda}{d\tau}\right)^{-1} = \frac{[3\lambda^2 + 2u_1\lambda + u_2]}{-\lambda(\lambda^3 + u_1\lambda^2 + u_2\lambda)} + \frac{(2v_1\lambda + v_2)}{(v_1\lambda^2 + v_2\lambda)\lambda} - \frac{\tau}{\lambda},$$

$$\lambda = i\omega_0,$$

$$\left(\frac{d\lambda}{d\tau}\right)^{-1} = \frac{1}{\omega_0}\left[\frac{[-3\omega_0^2 + 2iu_1\omega_0 + u_2]}{(-\omega_0^3 + u_2\omega_0 + iu_1\omega_0^2)} + \frac{(2iv_1\omega_0 + v_2)}{(-v_2\omega_0 - iv_1\omega_0^2)} + i\tau\right],$$

$$\left(\frac{d\lambda}{d\tau}\right)^{-1} = \frac{1}{\omega_0}\left[\frac{(-3\omega_0^2 + 2iu_1\omega_0 + u_2)(-\omega_0^3 + u_2\omega_0 - iu_1\omega_0^2)}{(-\omega_0^3 + u_2\omega_0)^2 + (u_1\omega_0^2)^2} + \frac{(2iv_1\omega_0 + v_2)(-v_2\omega_0 + iv_1\omega_0^2)}{(v_2\omega_0)^2 + (v_1\omega_0^2)^2} + i\tau\right].$$

Now, real part of

$$\left(\frac{d\lambda}{d\tau}\right)^{-1} = \frac{1}{\omega_0}\left[\frac{(-3\omega_0^2 + u_2)(-\omega_0^3 + u_2\omega_0) + 2u_1\omega_0(u_1\omega_0^2)}{(-\omega_0^3 + u_2\omega_0)^2 + (u_1\omega_0^2)^2} + \frac{(-v_2^2\omega_0 + 2v_1\omega_0(v_1\omega_0^2))}{(v_2\omega_0)^2 + (v_1\omega_0^2)^2}\right],$$

i.e.,

$$(v_1\omega_0^2)^2 + (v_2\omega_0)^2 = (\omega_0^2u_1)^2 + (-\omega_0^3 + \omega_0u_2)^2.$$

Which imply real part of

$$\left(\frac{d\lambda}{d\tau}\right)^{-1} = \frac{1}{\omega_0}\left[\frac{3\omega_0^5 + \omega_0^3(2u_1^2 - u_2 - 3u_2 - 2v_1^2) + (u_2^2 - v_2^2)\omega_0}{(v_2\omega_0)^2 + (v_1\omega_0^2)^2}\right],$$

i.e.,

$$\mathrm{Re}\left(\frac{d\lambda}{d\tau}\right)^{-1} = \left[\frac{3\omega_0^4 + \omega_0^2(2u_1^2 - 4u_2 - 2v_1^2) + (u_2^2 - v_2^2)}{(v_2\omega_0)^2 + (v_1\omega_0^2)^2}\right]$$

or

$$\left[\frac{d}{d\tau}\,\mathrm{Re}(\lambda)\right] = \left[\mathrm{Re}\left(\frac{d\lambda}{d\tau}\right)^{-1}\right]_{\lambda=i\omega_0} = \left[\frac{3\omega_0^4 + \omega_0^2(2u_1^2 - 4u_2 - 2v_1^2) + (u_2^2 - v_2^2)}{(v_2\omega_0)^2 + (v_1\omega_0^2)^2}\right] if\, u_1^2 - 2u_2 - v_1^2 > 0 \text{ and } u_2^2 - v_2^2 > 0.$$

Then

$$\left[\frac{d}{d\tau}\,\mathrm{Re}(\lambda)\right]_{\lambda=i\omega_0} > 0.$$

Therefore, the transversality condition holds and Hopf-bifurcation occurs at $\tau = \tau_0$. This τ_0 is called critical time delay parameter from which the system becomes unstable to stable. □

6. Numerical Simulation

Numerical simulations of the system provides visual insight into the stability at the equilibrium points. These graphs reveal critical thresholds where disease dynamics shift, guiding interventions. By analyzing bifurcation points, we can predict disease persistence or eradication under varying conditions. These graphs help analyze how disease prevalence changes over time, revealing whether the disease will persist or fade. Such simulations guide decision-making in public health interventions and outbreak management.

In this section, numerical simulation for different sets of parametric values is carried out using MATLAB. Twenty four examples (see Examples 6.1-6.24) are considered to analyse and ascertain our results. For all the examples, fixed populations $N = 60$, $S = 25$, $I = 31$, $R = 4$ are considered. The following examples (see Examples 6.1-6.12) illustrates the existence of the critical time delay parameter τ_0 (bifurcation point) for three sets of parametric values in which the transmission rate β, recovery rate γ varies separately or combinedly and the remaining parameters fixed constant.

Example 6.1. For $\beta = 0.02$, $\gamma = 0.5$, $\alpha = 0.7$, $\tau = 1.9 > \tau_0 = 1.82$, the time series response and phase portraits obtained through simulation, are shown in Figures 2 and 3.

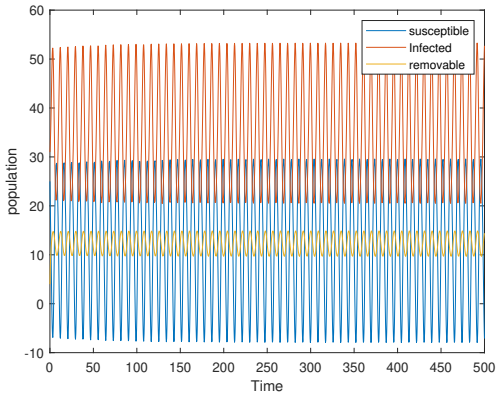

Figure 2. Demonstration of unstability of the system when $\tau = 1.9 > \tau_0 = 1.82$ in support of Theorem 5.1 by frequency response

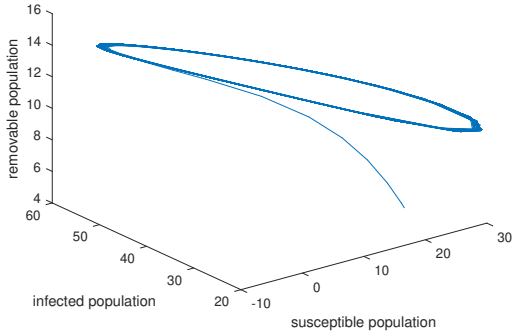

Figure 3. Demonstration of unstability of the system when $\tau = 1.9 > \tau_0 = 1.82$ in support of Theorem 5.1 by phase portraits

Example 6.2. For $\beta = 0.02$, $\gamma = 0.5$, $\alpha = 0.7$, $\tau = 1.85 > \tau_0 = 1.82$, the time series response and phase portraits obtained through simulation, are shown in Figures 4 and 5.

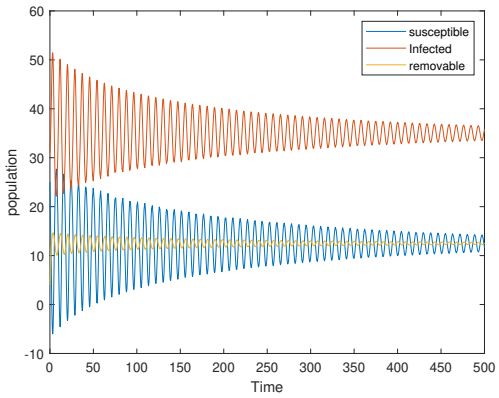

Figure 4. Demonstration of unstability of the system when $\tau = 1.85 > \tau_0 = 1.82$ in support of Theorem 5.1 by frequency response

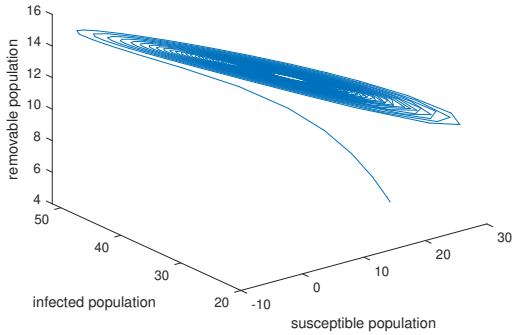

Figure 5. Demonstration of unstability of the system when $\tau = 1.85 > \tau_0 = 1.82$ in support of Theorem 5.1 by phase portraits

Example 6.3. For $\beta = 0.02$, $\gamma = 0.5$, $\alpha = 0.7$, the time series response and phase portraits obtained through simulation, are shown in Figures 6 and 7.

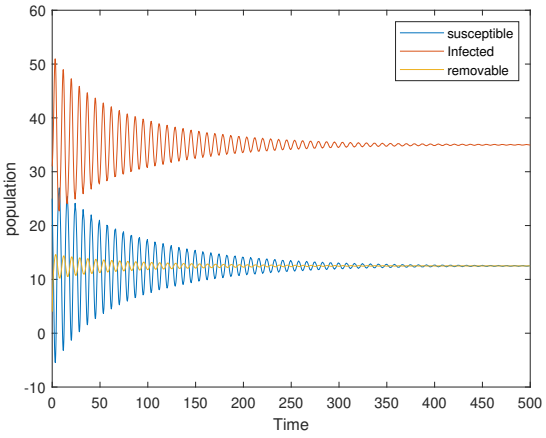

Figure 6. Demonstration of critical time delay parameter $\tau_0 = 1.82$ in support of Theorem 5.1 by frequency response

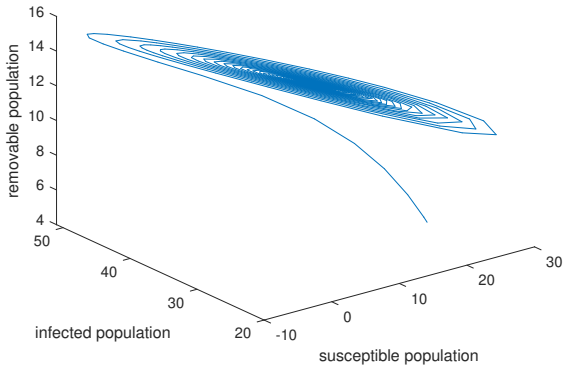

Figure 7. Demonstration of critical time delay parameter $\tau_0 = 1.82$ in support of Theorem 5.1 by phase portraits

Example 6.4. For $\beta = 0.02$, $\gamma = 0.5$, $\alpha = 0.7$, $\tau = 1.8 < \tau_0 = 1.82$, the time series response and phase portraits obtained through simulation, are shown in Figures 8 and 9.

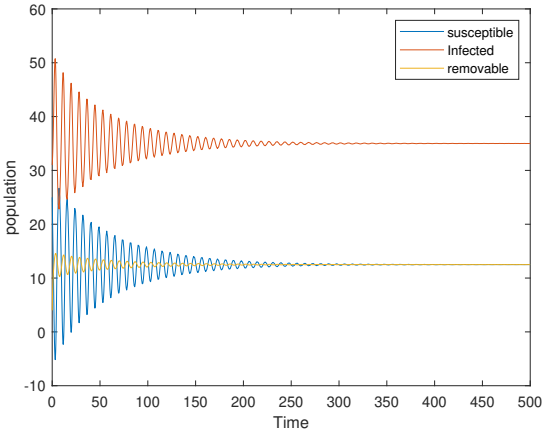

Figure 8. Demonstration of stability of the system when $\tau = 1.8 < \tau_0 = 1.82$ in support of Theorem 5.1 by frequency response

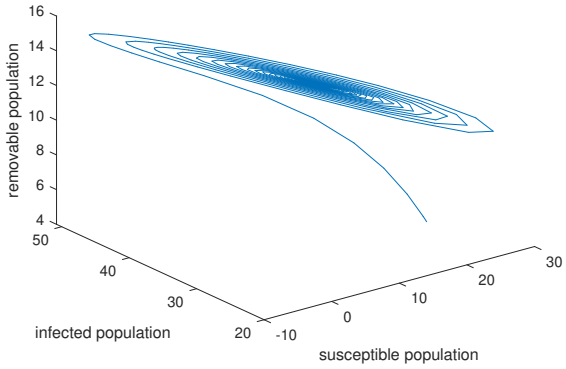

Figure 9. Demonstration of stability of the system when $\tau = 1.8 < \tau_0 = 1.82$ in support of Theorem 5.1 by phase portraits

In this case, the system converges to the fixed equilibrium point E(12,35,13) at $\tau = 1.8 < \tau_0 = 1.82$ and hence asymptotically stable. Thus, the Examples 6.1-6.4, illustrates the existence of the critical time delay parameter τ_0 and it is identified as 1.82.

Example 6.5. For $\beta = 0.018$, $\gamma = 0.3$, $\alpha = 0.7$, $\tau = 1.9 > \tau_0 = 1.78$, the time series response and phase portraits obtained through simulation, are shown in Figures 10 and 11.

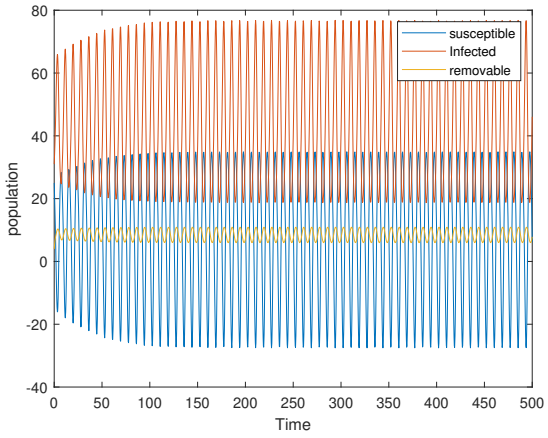

Figure 10. Demonstration of unstability of the system when $\tau = 1.9 > \tau_0 = 1.78$ in support of Theorem 5.1 by frequency response

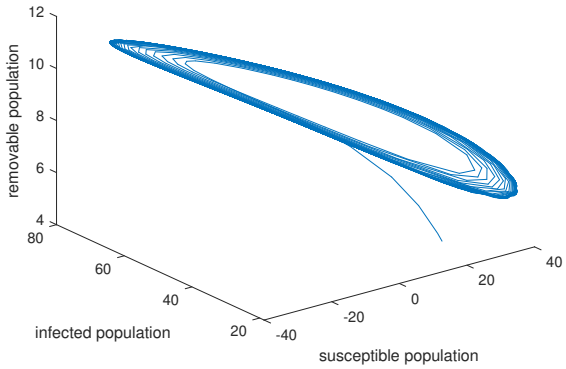

Figure 11. Demonstration of unstability of the system when $\tau = 1.9 > \tau_0 = 1.78$ in support of Theorem 5.1 by phase portraits.

Example 6.6. For $\beta = 0.018$, $\gamma = 0.3$, $\alpha = 0.7$, $\tau = 1.8 > \tau_0 = 1.78$, the time series response and phase portraits obtained through simulation, are shown in Figures 12 and 13.

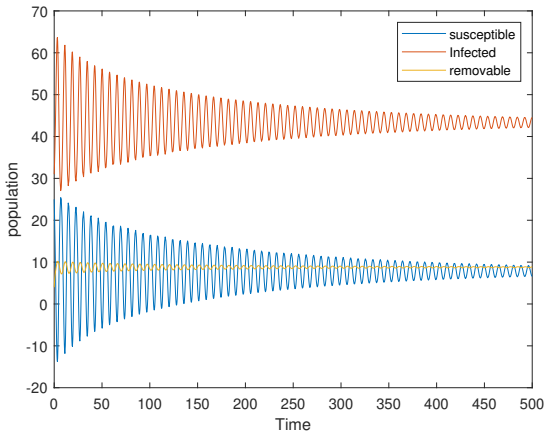

Figure 12. Demonstration of unstability of the system when $\tau = 1.8 > \tau_0 = 1.78$ in support of Theorem 5.1 by frequency response

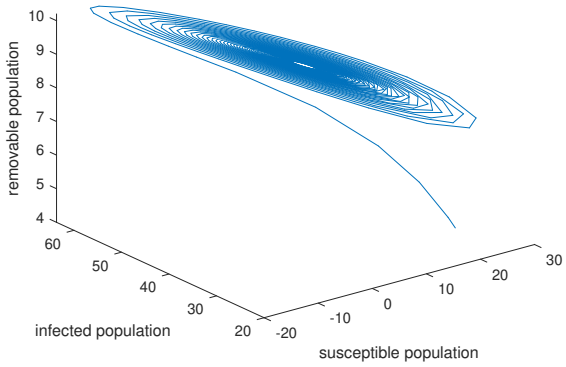

Figure 13. Demonstration of unstability of the system when $\tau = 1.8 > \tau_0 = 1.78$ in support of Theorem 5.1 by phase portraits

Example 6.7. For $\beta = 0.018$, $\gamma = 0.3$, $\alpha = 0.7$, the time series response and phase portraits obtained through simulation, are shown in Figures 14 and 15.

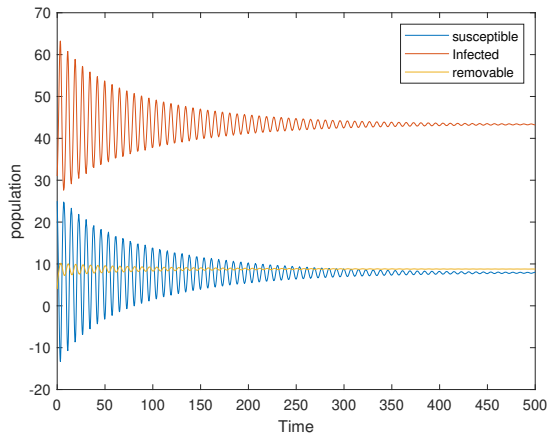

Figure 14. Demonstration of critical time delay parameter $\tau_0 = 1.78$ in support of Theorem 5.1 by frequency response

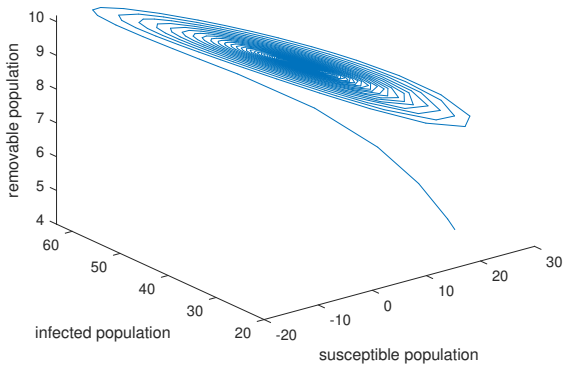

Figure 15. Demonstration of critical time delay parameter $\tau_0 = 1.78$ in support of Theorem 5.1 by phase portraits

Example 6.8. For $\beta = 0.018$, $\gamma = 0.3$, $\alpha = 0.7$, $\tau = 1.75 < \tau_0 = 1.78$, the time series response and phase portraits obtained through simulation, are shown in Figures 16 and 17.

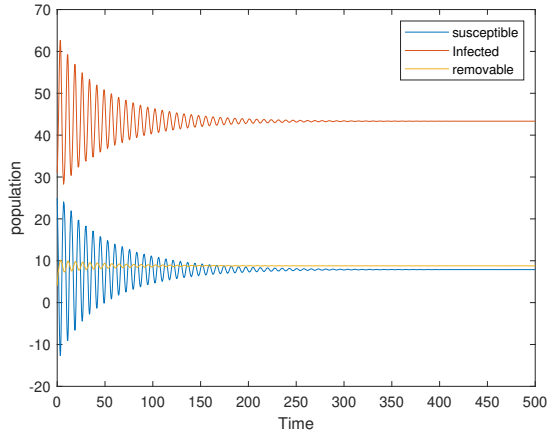

Figure 16. Demonstration of stability of the system when $\tau = 1.75 < \tau_0 = 1.78$ in support of Theorem 5.1 by frequency response.

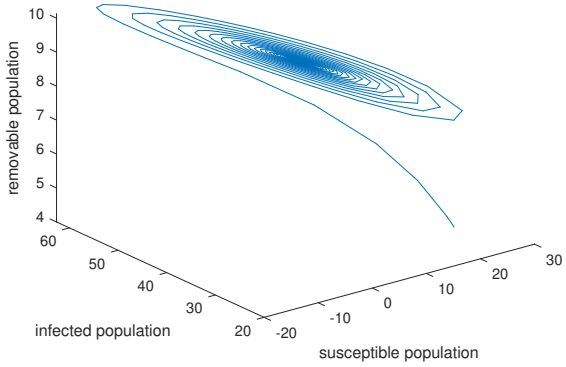

Figure 17. Demonstration of stability of the system when $\tau = 1.75 < \tau_0 = 1.78$ in support of Theorem 5.1 by phase portraits

From Figures 16 and 17, observe that the system converges to the fixed equilibrium point E(8,43,9) at $\tau = 1.75 < \tau_0 = 1.78$ and hence asymptotically stable. Thus, the Examples 6.5-6.8, illustrates the existence of the critical time delay parameter τ_0 and it is identified as 1.78.

Example 6.9. For $\beta = 0.02$, $\gamma = 0.3$, $\alpha = 0.7$, $\tau = 1.78 > \tau_0 = 1.57$, the time series response and phase portraits obtained through simulation, are shown in Figures 18 and 19.

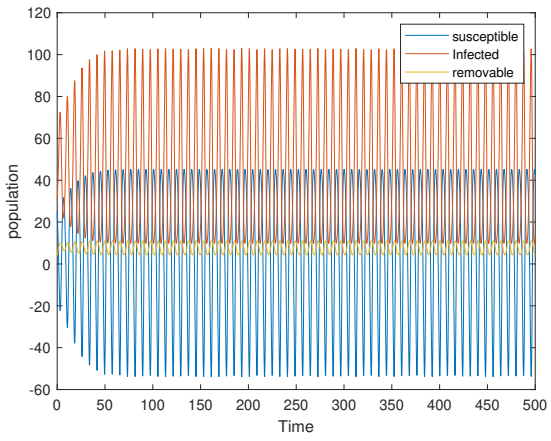

Figure 18. Demonstration of unstability of the system when $\tau = 1.78 > \tau_0 = 1.57$ in support of Theorem 5.1 by frequency response

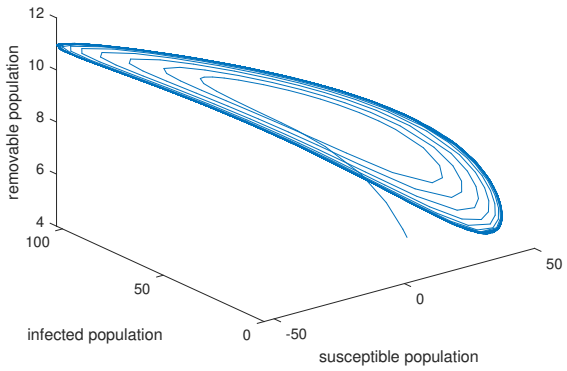

Figure 19. Demonstration of unstability of the system when $\tau = 1.78 > \tau_0 = 1.57$ in support of Theorem 5.1 by phase portraits

Example 6.10. For $\beta = 0.02$, $\gamma = 0.3$, $\alpha = 0.7$, $\tau = 1.62 > \tau_0 = 1.57$, the time series response and phase portraits obtained through simulation, are shown in Figures 20 and 21.

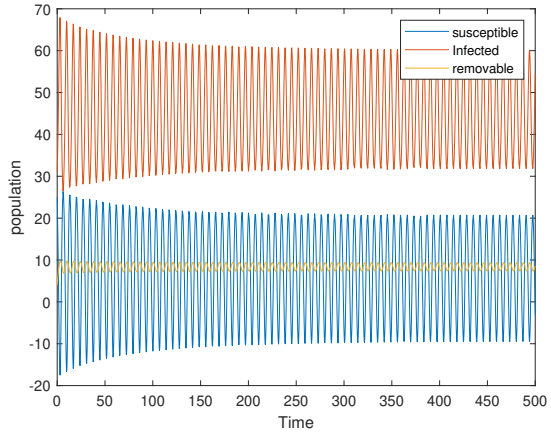

Figure 20. Demonstration of unstability of the system when $\tau = 1.62 > \tau_0 = 1.57$ in support of Theorem 5.1 by frequency response

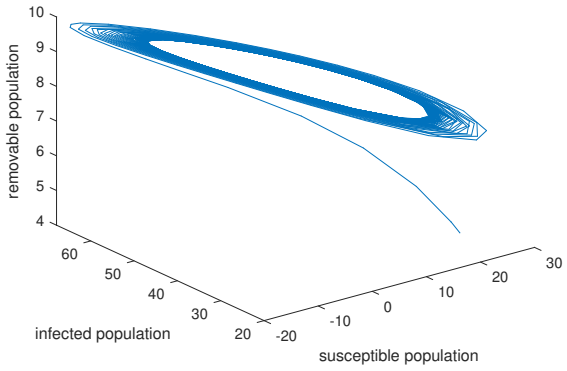

Figure 21. Demonstration of unstability of the system when $\tau = 1.62 > \tau_0 = 1.57$ in support of Theorem 5.1 by phase portraits

Example 6.11. For $\beta = 0.02$, $\gamma = 0.3$, $\alpha = 0.7$, the time series response and phase portraits obtained through simulation, are shown in Figures 22 and 23.

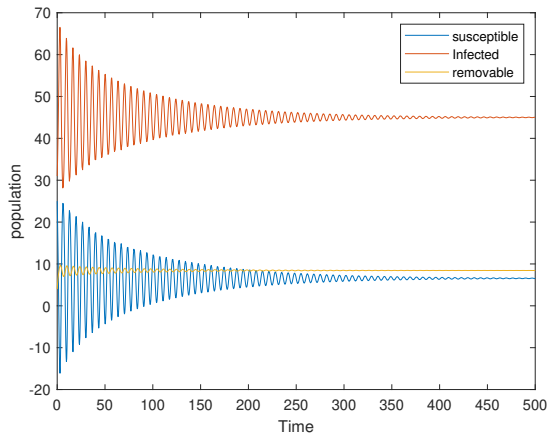

Figure 22. Demonstration of critical time delay parameter $\tau_0 = 1.57$ in support of Theorem 5.1 by frequency response

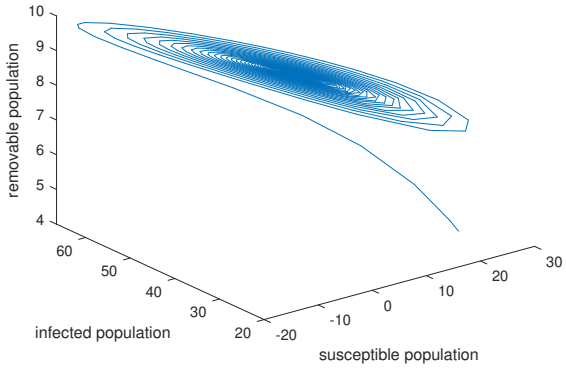

Figure 23. Demonstration of critical time delay parameter $\tau_0 = 1.57$ in support of Theorem 5.1 by phase portraits

Example 6.12. For $\beta = 0.02$, $\gamma = 0.3$, $\alpha = 0.7$, $\tau = 1.5 < \tau_0 = 1.57$, the time series response and phase portraits obtained through simulation, are shown in Figures 24 and 25.

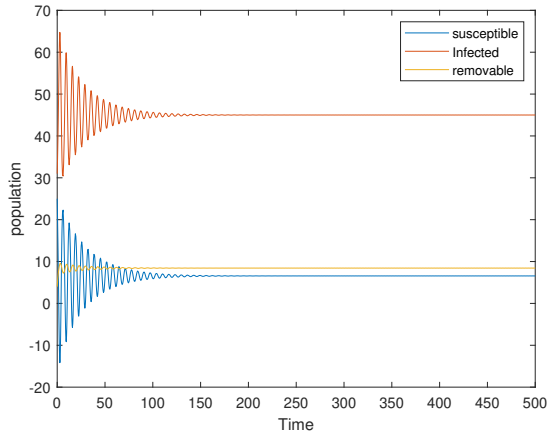

Figure 24. Demonstration of stability of the system when $\tau = 1.5 < \tau_0 = 1.57$ in support of Theorem 5.1 by frequency response

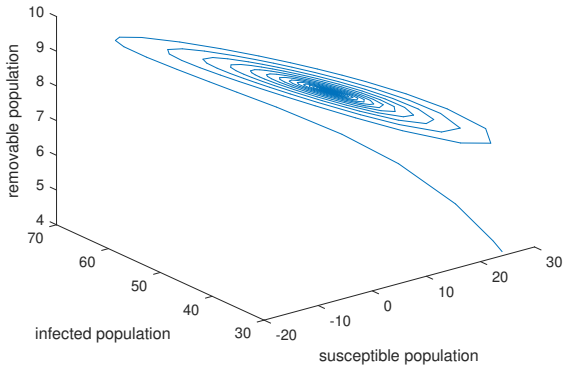

Figure 25. Demonstration of stability of the system when $\tau = 1.5 < \tau_0 = 1.57$ in support of Theorem 5.1 by phase portraits

From Figures 24 and 25, observe that the system converges to the fixed equilibrium point E(7,45,8) at $\tau = 1.5 < \tau_0 = 1.57$ and hence asymptotically stable. Thus, the Examples 6.9-6.12, illustrates the existence of the critical time delay parameter τ_0 and it is identified as 1.57.

The parametric values and the corresponding critical time delay parameters (bifurcation points) are tabulated in the Table 3.

S. No.	Example	Parametric Values	Critical Bifurcation Parameter (τ_0)
1	6.1-6.4	$\beta = 0.02, \gamma = 0.5, \alpha = 0.7$	$\tau_0 = 1.82$
2	6.5-6.8	$\beta = 0.018, \gamma = 0.3, \alpha = 0.7$	$\tau_0 = 1.78$
3	6.9-6.12	$\beta = 0.02, \gamma = 0.3, \alpha = 0.7$	$\tau_0 = 1.57$

Table 3. Critical time delay parameters for different sets of parametric values

For the above three sets of parametric values, the critical time delay parameter τ_0 evaluated theoretically and it is observed that the obtained values are closure to the values obtained graphically. The corresponding values are tabulated in the Table 4.

Parameters	$\beta = 0.02, \gamma = 0.5, \alpha = 0.7$	$\beta = 0.018, \gamma = 0.3, \alpha = 0.7$	$\beta = 0.02, \gamma = 0.3, \alpha = 0.7$
u_1	1.4	1.468	1.6
u_2	-0.168	-0.115656	-0.126
v_1	0.7	0.774	0.9
v_2	1.148	1.247688	1.4512
N_1	1.806	1.78726	2.002
N_2	-1.28968	-1.54335	-2.089525
ω_0	0.74	0.8	0.872
τ_0 (Theoretical)	1.87	2.01	1.34
τ_0 (Graphical)	1.82	1.78	1.57

Table 4. Comparison of theoretical and graphical values of critical time delay parameter τ_0

In the following examples (see Examples 6.13 and 6.14), considered two sets of parametric values in which the transmission rate β is varied to ascertain the unstability of the system at fixed critical time delay parameter τ_0.

Example 6.13. For $\beta = 0.018$, $\gamma = 0.5$, $\alpha = 0.05$, the time series response and phase portraits obtained through simulation, are shown in Figures 26 and 27.

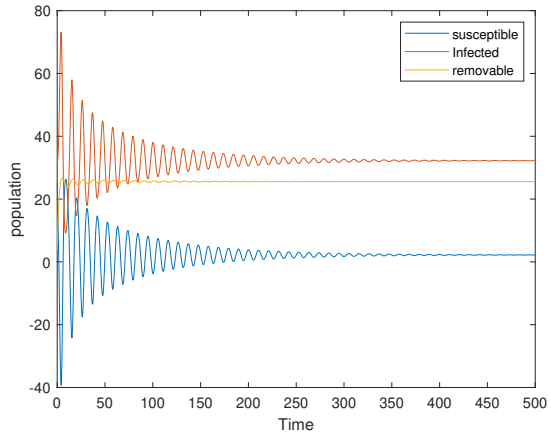

Figure 26. Demonstration of how β influences the stability of the system when $\beta = 0.018$ at critical time delay parameter $\tau_0 = 2.49$ by frequency response.

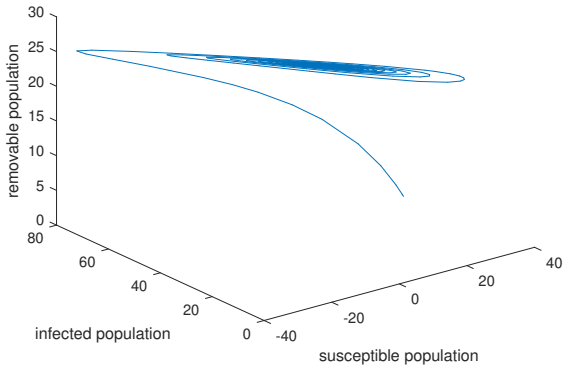

Figure 27. Demonstration of how β influences the stability of the system when $\beta = 0.018$ at critical time delay paramter $\tau_0 = 2.49$ by phase portraits.

Example 6.14. For $\beta = 0.019$, $\gamma = 0.5$, $\alpha = 0.05$, $\tau_0 = 2.49$, the time series response and phase portraits obtained through simulation, are shown in Figures 28 and 29.

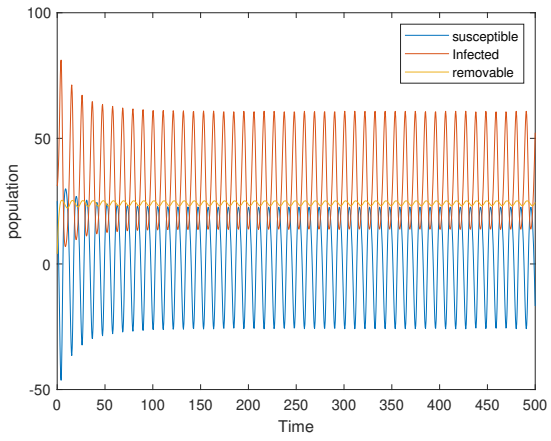

Figure 28. Demonstration of how β influences the stability of the system when $\beta = 0.019$ at critical time delay parameter $\tau_0 = 2.49$ by frequency response

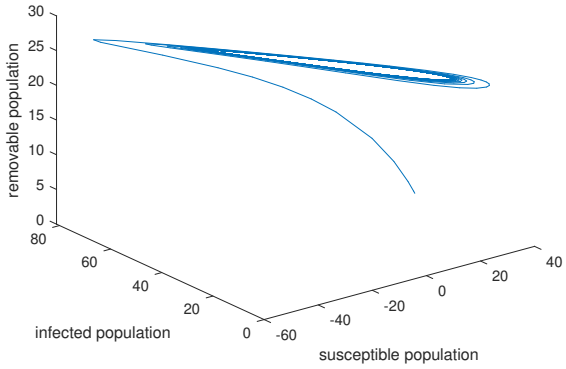

Figure 29. Demonstration of how β influences the stability of the system when $\beta = 0.019$ at critical time delay parameter $\tau_0 = 2.49$ by phase portraits

Example 6.15. For $\beta = 0.02$, $\gamma = 0.5$, $\alpha = 0.05$, $\tau_0 = 2.49$, the time series response and phase portraits obtained through simulation, are shown in Figures 30 and 31.

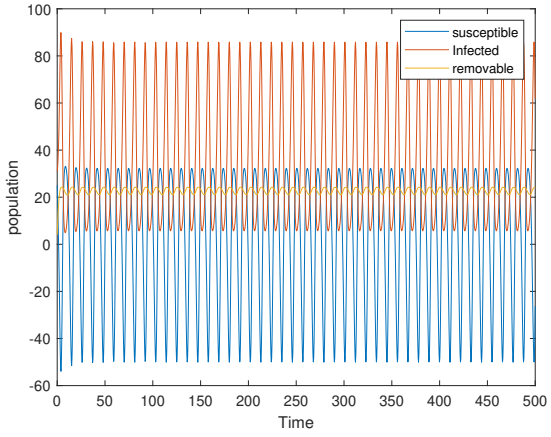

Figure 30. Demonstration of how β influences the stability of the system when $\beta = 0.02$ at critical time delay parameter $\tau_0 = 2.49$ by frequency response.

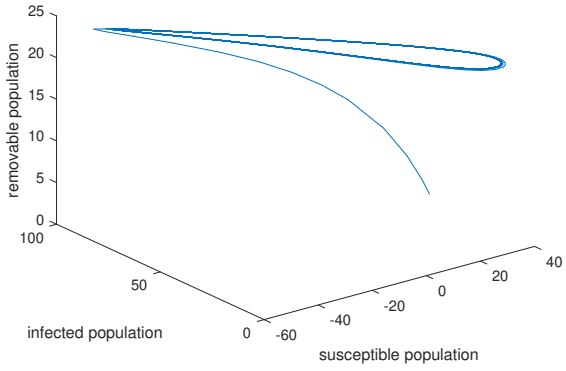

Figure 31. Demonstration of how β influences the stability of the system when $\beta = 0.02$ at critical time delay parameter $\tau_0 = 2.49$ by phase portraits.

From the Examples 6.13-6.15, it is observed that when the transmission rate (β) is increased at critical time delay parameter $\tau_0 = 2.49$, the system becomes unstable.

Example 6.16. For $\beta = 0.015$, $\gamma = 0.3$, $\alpha = 0.7$, the time series response and phase portraits obtained through simulation, are shown in Figures 32 and 33.

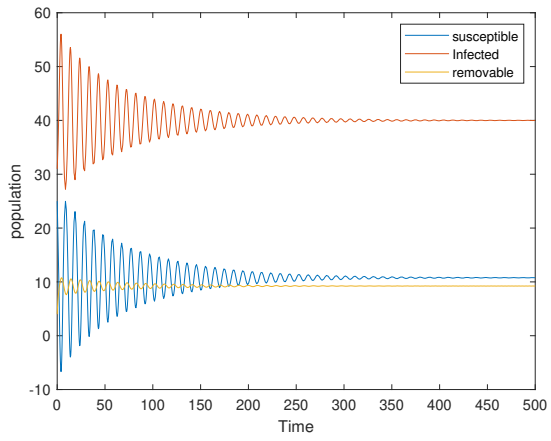

Figure 32. Demonstration of how β influences the stability of the system when $\beta = 0.015$ at critical time delay parameter $\tau_0 = 2.2$ by frequency response

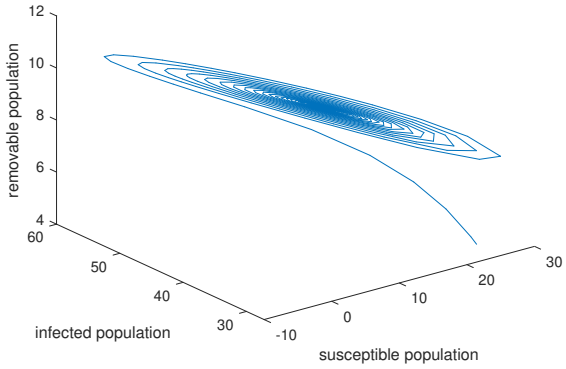

Figure 33. Demonstration of how β influences the stability of the system when $\beta = 0.015$ at critical time delay parameter $\tau_0 = 2.2$ by phase portraits

Example 6.17. For $\beta = 0.016$, $\gamma = 0.3$, $\alpha = 0.7$, $\tau_0 = 2.2$, the time series response and phase portraits obtained through simulation, are shown in Figures 34 and 35.

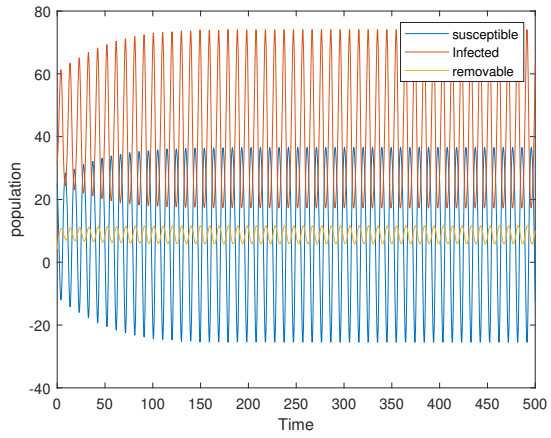

Figure 34. Demonstration of how β influences the stability of the system when $\beta = 0.016$ at critical time delay parameter $\tau_0 = 2.2$ by frequency response

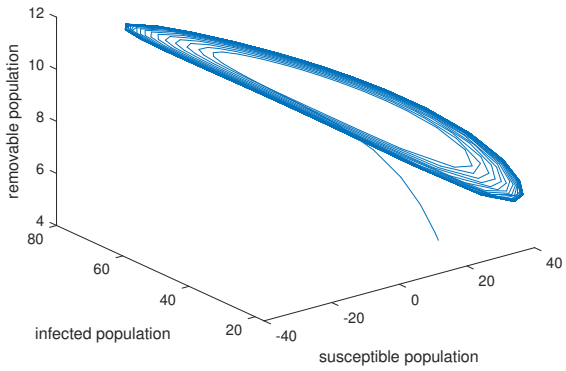

Figure 35. Demonstration of how β influences the stability of the system when $\beta = 0.016$ at critical time delay parameter $\tau_0 = 2.2$ by phase portraits

Example 6.18. For $\beta = 0.017$, $\gamma = 0.3$, $\alpha = 0.7$, $\tau_0 = 2.2$, the time series response and phase portraits obtained through simulation, are shown in Figures 36 and 37.

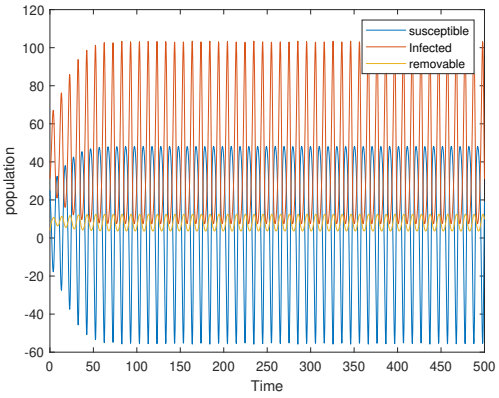

Figure 36. Demonstration of how β influences the stability of the system when $\beta = 0.017$ at critical time delay parameter $\tau_0 = 2.2$ by frequency response

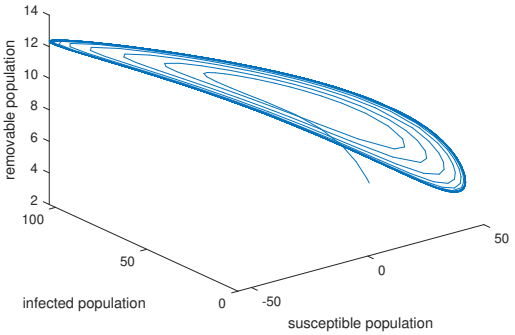

Figure 37. Demonstration of how β influences the stability of the system when $\beta = 0.017$ at critical time delay parameter $\tau_0 = 2.2$ by phase portraits

From the Examples 6.16-6.18, it is observed that when the transmission rate (β) is increased at critical time delay parameter $\tau_0 = 2.2$, the system becomes unstable.

The parametric values and the corresponding transmission rate (β) are tabulated in the Table 5.

S. No.	Example	Parametric Values	β	Observation
1	6.13	$\gamma = 0.5, \alpha = 0.05, \tau_0 = 2.49$	0.018	$\tau_0 = 2.49$
2	6.14	$\gamma = 0.5, \alpha = 0.05, \tau_0 = 2.49$	0.019	unstable
3	6.15	$\gamma = 0.5, \alpha = 0.05, \tau_0 = 2.49$	0.02	unstable
4	6.16	$\gamma = 0.3, \alpha = 0.7, \tau_0 = 2.2$	0.015	$\tau_0 = 2.2$
5	6.17	$\gamma = 0.3, \alpha = 0.7, \tau_0 = 2.2$	0.016	unstable
6	6.18	$\gamma = 0.3, \alpha = 0.7, \tau_0 = 2.2$	0.017	unstable

Table 5. Table displaying the impact of the transmission rate β on the delay

Two sets of parametric values is considered in which the additional transaction rate α is varied to ascertain the unstability of the system at fixed critical time delay parameter τ_0 in the Examples 6.19-6.24.

Example 6.19. For $\beta = 0.02$, $\gamma = 0.5$, $\alpha = 0.3$, the time series response and phase portraits obtained through simulation, are shown in Figures 38 and 39.

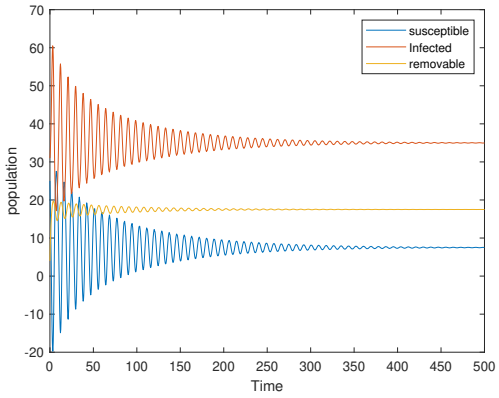

Figure 38. Demonstration of how α influences the stability of the system when $\alpha = 0.3$ at critical time delay parameter $\tau_0 = 1.92$ by frequency response

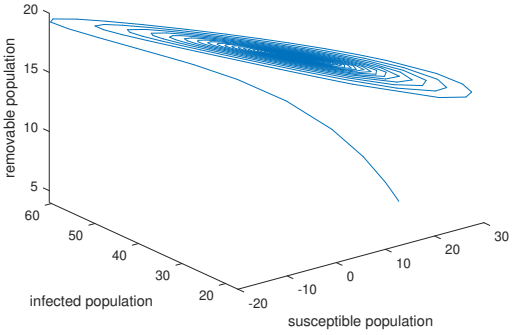

Figure 39. Demonstration of how α influences the stability of the system when $\alpha = 0.3$ at critical time delay parameter $\tau_0 = 1.92$ by phase portraits

Example 6.20. For $\beta = 0.02$, $\gamma = 0.5$, $\alpha = 0.5$, $\tau_0 = 1.92$, the time series response and phase portraits obtained through simulation, are shown in Figures 40 and 41.

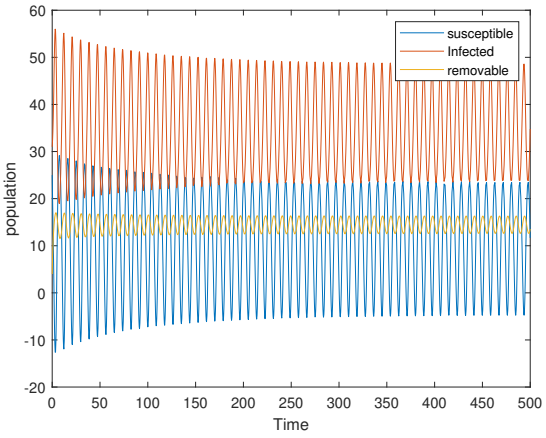

Figure 40. Demonstration of how α influences the stability of the system when $\alpha = 0.5$ at critical time delay parameter $\tau_0 = 1.92$ by frequency response

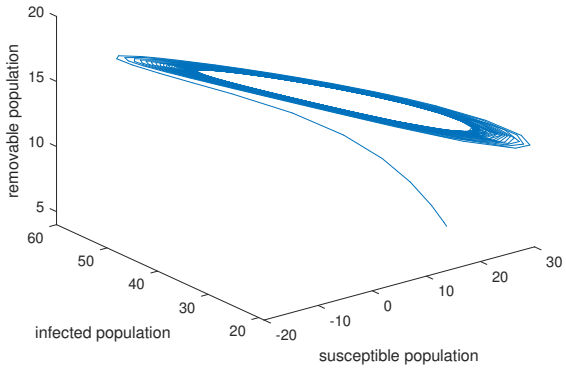

Figure 41. Demonstration of how α influences the stability of the system when $\alpha = 0.5$ at critical time delay parameter $\tau_0 = 1.92$ by phase portraits

Example 6.21. For $\beta = 0.02$, $\gamma = 0.5$, $\alpha = 0.7$, $\tau_0 = 1.92$, the time series response and phase portraits obtained through simulation, are shown in Figures 42 and 43.

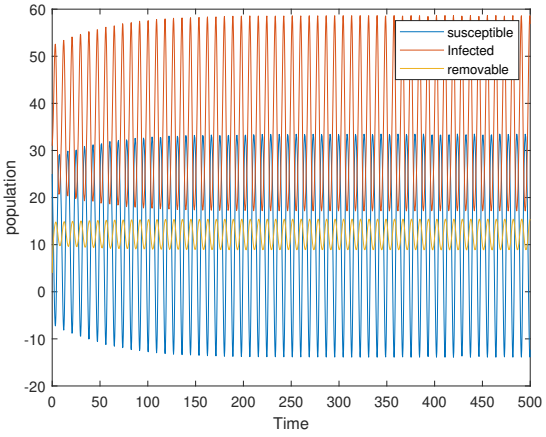

Figure 42. Demonstration of how α influences the stability of the system when $\alpha = 0.7$ at critical time delay parameter $\tau_0 = 1.92$ by frequency response

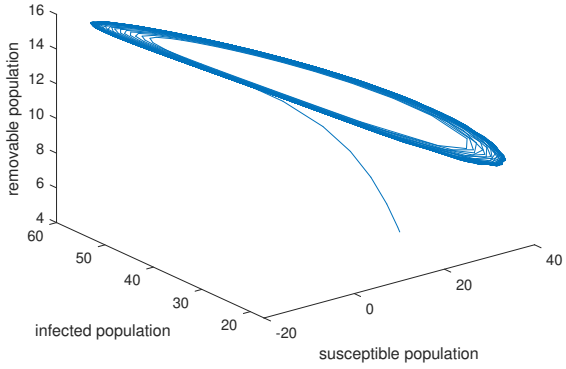

Figure 43. Demonstration of how α influences the stability of the system when $\alpha = 0.7$ at critical time delay parameter $\tau_0 = 1.92$ by phase portraits

In Examples 6.19 to 6.21, it is observed that as the additional transition rate α increases at the critical time delay parameter $\tau_0 = 1.92$, the system becomes unstable.

Example 6.22. For $\beta = 0.018$, $\gamma = 0.3$, $\alpha = 0.05$, the time series response and phase portraits obtained through simulation, are shown in Figures 44 and 45.

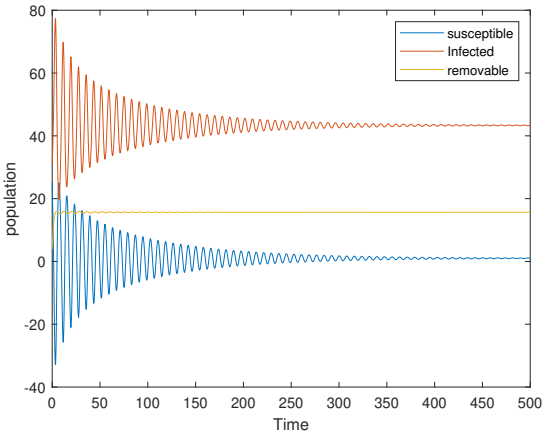

Figure 44. Demonstration of how α influences the stability of the system when $\alpha = 0.05$ at critical time delay parameter $\tau_0 = 1.93$ by frequency response

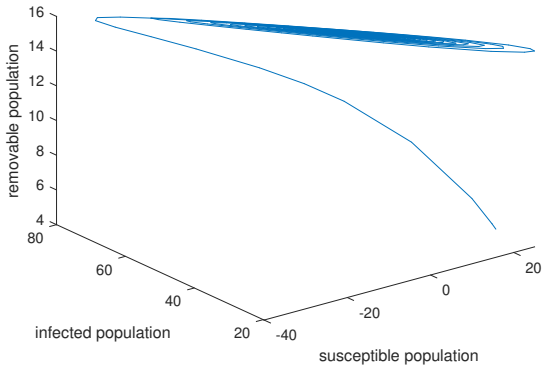

Figure 45. Demonstration of how α influences the stability of the system when $\alpha = 0.05$ at critical time delay parameter $\tau_0 = 1.93$ by phase portraits

Example 6.23. For $\beta = 0.018$, $\gamma = 0.3$, $\alpha = 0.1$, $\tau_0 = 1.93$, the time series response and phase portraits obtained through simulation, are shown in Figures 46 and 47.

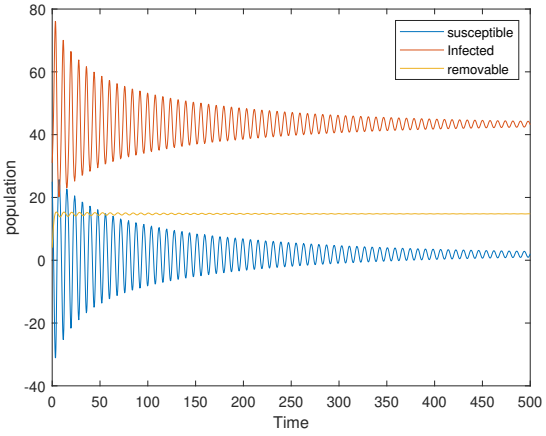

Figure 46. Demonstration of how α influences the stability of the system when $\alpha = 0.1$ at critical time delay parameter $\tau_0 = 1.93$ by frequency response.

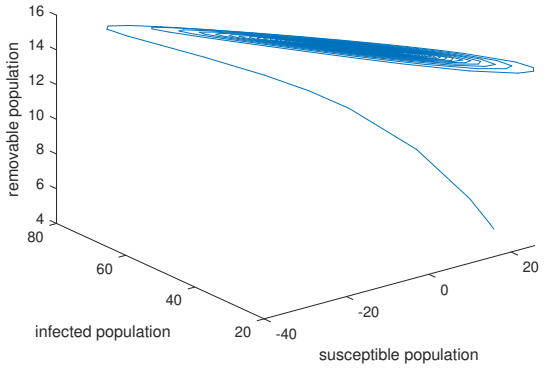

Figure 47. Demonstration of how α influences the stability of the system when $\alpha = 0.1$ at critical time delay parameter $\tau_0 = 1.93$ by phase portraits.

Example 6.24. For $\beta = 0.018$, $\gamma = 0.3$, $\alpha = 0.15$, $\tau_0 = 1.93$, the time series response and phase portraits obtained through simulation, are shown in Figures 48 and 49.

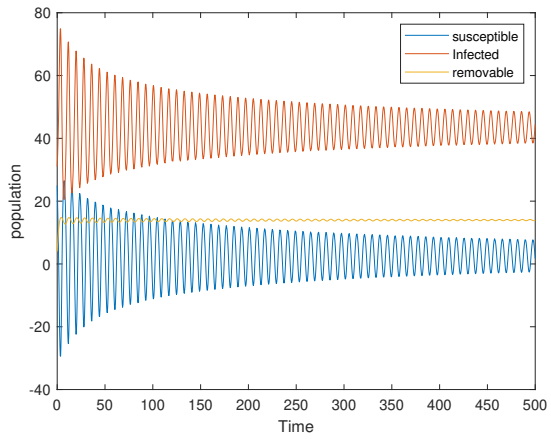

Figure 48. Demonstration of how α influences the stability of the system when $\alpha = 0.15$ at critical time delay parameter $\tau_0 = 1.93$ by frequency response.

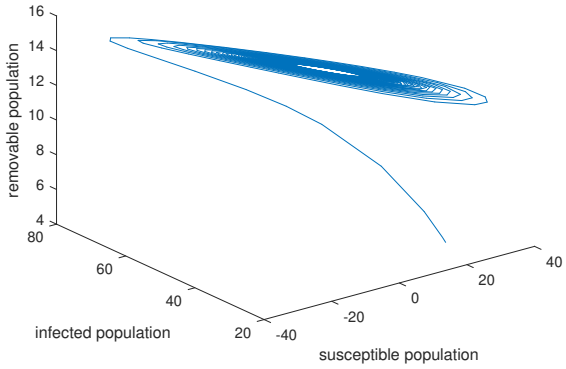

Figure 49. Demonstration of how α influences the stability of the system when $\alpha = 0.15$ at critical time delay parameter $\tau_0 = 1.93$ by phase portraits

In Examples 6.22-6.24, it is observed that as the additional transition rate α increases at the critical time delay parameter $\tau_0 = 1.93$, the system becomes unstable.

The parametric values and the corresponding to the additional transaction rate (α) is increases are tabulated in the Table 6.

S. No.	Example	Parametric Values	α	Observation
1	6.19	$\beta = 0.02, \gamma = 0.5, \tau_0 = 1.92$	0.3	$\tau_0 = 1.92$
2	6.20	$\beta = 0.02, \gamma = 0.5, \tau_0 = 1.92$	0.5	unstable
3	6.21	$\beta = 0.02, \gamma = 0.5, \tau_0 = 1.92$	0.7	unstable
4	6.22	$\beta = 0.018, \gamma = 0.3, \tau_0 = 1.93$	0.05	$\tau_0 = 1.93$
5	6.23	$\beta = 0.018, \gamma = 0.3, \tau_0 = 1.93$	0.1	unstable
6	6.24	$\beta = 0.018, \gamma = 0.3, \tau_0 = 1.93$	0.15	unstable

Table 6. Table illustrating the impact of the additional transition rate α on the delay

7. Results and conclusions

A three-compartment SIRI epidemic model with reintroduced susceptibles (i.e., SIR$\begin{smallmatrix}/\text{I}\\ \backslash\text{S}\end{smallmatrix}$) under incorporated time delay on susceptible individuals is considered. It is observed that the model admits a disease free equilibrium point if the basic reproductive rate is less than one. Also the system admits an endemic equilibrium point, if the basic reproductive rate is greater than one and from Theorem 4.1 the system is locally asymptotically stable if $2I^* > N$. Numerical simulation is carried out by considering twenty four examples to support the results using MATLAB. Obtained bifurcation points for three different sets of parametric values subject to variation in the transmission rate β and recovery rate γ and the remaining parameters fixed constant. Also considered two sets of parametric values to observe the effect of transmission rate β on delay and observed that when the transmission rate β is varied the system is becoming unstable at fixed critical time delay parameter τ_0. Further, considered two sets of parametric values to observe the effect of additional transaction rate α on delay and observed that when the additional transaction rate α is varied the system is becoming unstable at fixed critical time delay parameter τ_0.

Acknowledgments

In honor of Professor Yilmaz SIMSEK's 60th birthday, this work is dedicated to him.

The authors appreciate the editors' and referees' thorough evaluation, guidance, and insightful remarks that helped the work get better.

Author Contributions: This work is part of the first author's Ph.D. thesis submission, and each author made an equal contribution to the research, writing, review, and editing.

Conflict of Interest: The authors say that they have no conflicts of interest.

Funding (Financial Disclosure): Funding is not available to support this work.

References

[1] T. David, *A deterministic model for herpes infections in human and animal populations*, SIAM Rev. **32 (1)**, 136–139, 1990.
[2] A. R. Dokala, K. V. Shaik and A. V. Paparao, *Dynamics of directly transmitted viral micro parasite model*, Int. J. Ecol. Dev. **32 (4)**, 88–97, 2017.
[3] A. R. Dokala, K. V. Shaik and A. V. Paparao, *Viral Micro parasite model with distributed delay with distributed delay*, i-manager's J. Math. **8 (2)**, 25–35, 2019.
[4] A. R. Dokala, K. V. Shaik and A. V. Paparao, *Dynamics of delayed SIRS model with a non-linear incidence rate*, i-manager's J. Math. **8 (3)**, 17–27, 2019.
[5] A. R. Dokala, K. V. Shaik and A. V. Paparao, *Stability of SIRS epidemic model with non linear incidence rate*, Sci. Spec. **5 (3)**, 118–126, 2020.
[6] A. R. Dokala, K. V. Shaik and A. V. Paparao, *Dynamics of SIRS epidemic model under saturated treatment*, Int. J. Ecol. Econ. Stat. **43 (3)**, 106–119, 2022.
[7] A. R. Dokala, K. V. Shaik and A. V. Paparao, *A Time delay viral Micro parasite model*, Int. J. Ecol. Dev. **37 (1)**, 73–87, 2022.
[8] K. M. L. Emandi, K. V. Shaik, A. R. Dokala and S. Umme, *Stability analysis of SIRI epidemic model with reintroduced susceptibles*, Afr. J. Bio. **6 (Si 4)**, 5212–5222, 2024.
[9] K. M. L. Emandi, K. V. Shaik, A. R. Dokala and S. Umme, *Stability analysis of SIR-I/S epidemic model with time delay in the interaction of susceptible and infected individuals*, J. Comput. Anal. Appl. (JoCAAA), **33 (6)**, 958–972, 2024.
[10] D. K. Gummala, K. V. Shaik, A. R. Dokala and S. Umme, *Stability analysis of SIR epidemic model under vaccination coverage on newborns with time delay in the interaction of Susceptible and infected individuals*, Afr. J. Bio. Sc. **6 (Si4)**, 5196–5211, 2024.
[11] D. K. Gummala, K. V. Shaik, A. R. Dokala and S. Umme, *Vaccination dynamics and stability insights- A SIR model approach to epidemic control*, J. Comput. Anal. Appl. (JoCAAA) **33 (7)**, 16–28, 2024.
[12] C. James, *Control of communicable diseases manual*, American Public Health Association, Washington, 1999.
[13] N. Stollenwerk and V. Jansen, *Population biology and criticality*, Imperical College Press, London, 2011.
[14] K. E. VanLandingham, H. B. Marsteller, G. W. Ross and F. G. Hayden, *Relapse of herpes simplex encephalitis after conventional acyclovir therapy*, JAMA **259**, 1051–1053, 1988.
[15] M. S. Wayne, *Livestock disease eradication: Evaluation of the cooperative state federal bovine tuberculosis eradication program*, National Academy Press, Washington, 1994.

How to cite this article: K. M. L. Emandi, K. V. Shaik, A. R. Dokala and S. Umme, *Stability analysis of SIRI epidemic model with reintroduced susceptibles under incorporated time delay on susceptible individuals*, Montes Taurus J. Pure Appl. Math. **6 (3)**, 558–578, 2024; Article ID: MTJPAM-D-24-00155.